# INVESTIGATION OF HYPERSONIC INJECTION

R. CASEY and R.J. STALKER

Mechanical Engineering Department
University of Queensland, St. Lucia, Qld. 4067
AUSTRALIA

Abstract

Weinstein et al (1956) proposed a model for the diffusion of momentum from a slot jet into a moving secondary medium which dealt with isothermal incompressible flows. In this paper the model will be extended to encompass compressible flows by incorporating the Howarth transformation. The Schwarb Zeldovich transformations are then used to extend the model to combustion flows. This is then used to give a first order estimate of the combusting flow of a slot jet issuing into a free stream of nominal Mach number 3.5 which is compared to experimental results through interferograms. Results for predictions of similar flows at hypersonic Mach numbers (>5) are then presented.

## Introduction and Compressible Transformation

Weinstein et al (1956) conducted a series of experiments on the mixing of two co-flowing streams of air. A 1/2 in. x 12 in. cross section injector issued air into a larger chamber which was 10 3/4 in. x 12 in. The air was at a sufficiently low velocity to assume incompressibility of both streams and the length to width ratio of the injector was 24:1 so as to validate the assumption of two dimensionality. It was found that the variable of primary importance was the ratio of the injected air velocity to the free stream air velocity and not the absolute air velocities and hence the experiments were run for 3 different values of this parameter. The experimental results were compared to some experimental results obtained by Forthmann (1934) for a jet issuing into a quiescent free stream.

The model proposed by Weinstein et al (1956) was for a fluid which was incompressible and isothermal. Moreover it assumed that the flow was turbulent however no mathematical turbulence model was used to describe the nature of the turbulence. Rather, an empirical fit to experimental data was used. As such, this should allow the model to be applied to other similar flows where an empirical fit can be determined. An extension to compressible flows can be obtained via the Howarth transformation where the incompressible flow field is mapped to the compressible flow field according to the coordinate system given below in equations 1-4. This is basically a stretching/shrinking of the y coordinate of the flow field to allow for density variations. The tiltered variables correspond to the compressible flow field.[1]

$$\hat{dx} = dx \qquad \text{— [1]}$$

$$\hat{dy} = (\rho(x,y)/\rho_\infty)\, dy \qquad \text{— [2]}$$

$$\hat{u} = u \qquad \text{— [3]}$$

$$\hat{v} = \rho/\rho_\infty\, v + u\int_0^y \frac{\partial}{\partial x}(\rho/\rho_\infty)\, dy \qquad \text{— [4]}$$

This flow field can be further extended by incorporating the Schwarb Zeldovich transformations to give a first order model of combustion. Inherent in these transformations is the assumption that the Lewis number and the Prandtl number are unity which would not be true for most experiments however it suffices as a "first guess". Moreover the Schwarb Zeldovich transformations rely on the similarity of the conservation equations and their respective boundary conditions for momentum, heat and mass transfer so that the solution to the heat and mass transfer problem will be a linear function of the momentum diffusion solution. Similarly, the species concentration problem in the Schwarb Zeldovich transformations is formulated so that there is again similarity in the governing conservation equations and boundary conditions so that the species concentration solution will be a linear function of the momentum diffusion solution. Thus by considering the simple reaction scheme of f kg of fuel plus 1 kg of oxygen producing 1+f kg of products plus f $\Delta H$ kJ heat, solutions to the species concentration problem can be found from eq.(5) below where b is the Schwarb Zeldovich variable and i = 1,2,3 for fuel, oxygen or products respectively

$$b_i = c_1 + c_2 u \qquad \text{— [5]}$$

and the constants are found from matching the solution to the boundary conditions. Similarly the combustion temperature profiles can be found.[1]

[1] See Kanury (1975) for a more descriptive explanation

## Momentum Diffusion Model

Fig. 1 shows the flow field described by the 2 dimensional model. It is assumed that free mixing takes place between the two streams resulting in the conservation of relative momentum at every downstream station where the relative momentum is given by

$$\rho[u_\infty - u(x,y)]^2 \qquad -[6]$$

Furthermore, the diffusion of relative momentum in the mixing region is assumed to be Gaussian so that

$$\rho[u_\infty - u(x,y)]^2 = k(x)\ \exp-(y/b(x))^2 \qquad -[7]$$

where k(x) and b(x) represent the spread of the mixing region as the downstream distance is varied. Finally, the effusion of momentum from the injector is assumed to be made up of the superposition of individual point sources of momentum. Therefore integrating over the exit of the injector and applying the constraint of conservation of momentum, eq. (8) is derived.

$$\frac{u^2 - u_\infty^2}{u_j^2 - u_\infty^2} = \frac{1}{2}\left\{ \operatorname{erf}\left[\frac{d}{2b}\left(\frac{2y}{d}+1\right)\right] - \operatorname{erf}\left[\frac{d}{2b}\left(\frac{2y}{d}-1\right)\right]\right\} \qquad -[8]$$

where erf is the error function and d is the jet width as shown in fig.1. The function notation for b(x) is written as b for simplicity. By neglecting velocity fluctuations and then rearranging terms yeilds

$$\frac{u - u_\infty}{u_j - u_\infty} = \left\{\left(\frac{1}{2\epsilon}\right)^2 + \frac{1+\epsilon}{2\epsilon}\left[\operatorname{erf}\left[\frac{d}{2b}\left(\frac{2y}{d}+1\right)\right] - \operatorname{erf}\left[\frac{d}{2b}\left(\frac{2y}{d}-1\right)\right]\right]\right\}^{\frac{1}{2}} - \frac{1}{2\epsilon} \qquad -[9]$$

where

$$\epsilon = \frac{u_j - u_\infty}{2u_\infty}$$

which is constant for a given flow configuration.

This equation is devoid of all physical mixing parameters such as viscosity as this information is tied up in the spreading coefficient b.

The spreading coefficient is determined by considering the decay of centerline velocity ratio with distance. In this case, equation [9] reduces to

$$\frac{u_c - u_\infty}{u_j - u_\infty} = \left\{\left(\frac{1}{2\epsilon}\right)^2 + \left(\frac{1+\epsilon}{\epsilon}\right)\operatorname{erf}\left(\frac{d}{2b}\right)\right\}^{\frac{1}{2}} - \frac{1}{2\epsilon} \qquad -[10]$$

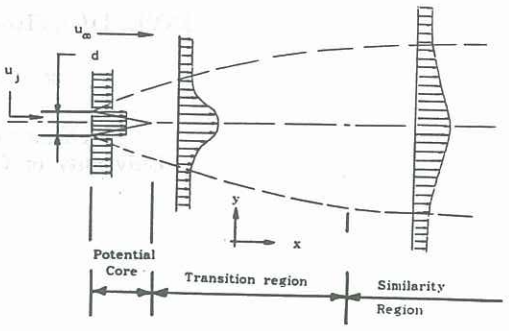


Figure 1 Two dimensional flow field

where the right hand side of [10] is a function of (d/2b) only for a given ε. Using this, Weinstein et al (1956) obtained the results of figure 2.

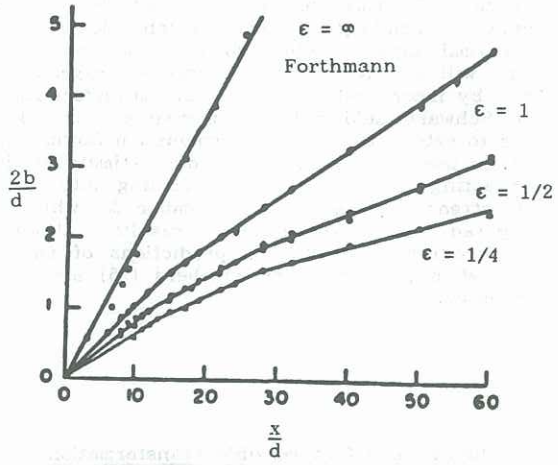


Figure 2 Spreading coefficient vrs. x
( From Weinstein )

## Prediction of Compressible Combustion Flows

The spreading coefficient variation with downstream distance for a given ε was approximated by a best fit hyperbolic function and the variation of the asymptote of the hyperbola with ε was approximated by a third order polynomial. Hence for any given value of ε and x/d , a value of b could be determined and therefore a velocity profile is specified by equation [9]. Having solved the velocity profile, the Schwarb Zeldovich transformations were applied to provide the species concentration and temperature information for the flow field. Then by summing the density times the relative mass fraction over the 4 species present,(with nitrogen as an inert dilutent gas) the Howarth transformation would give the compressible profile from the equations below,

$$\hat{dy} = \Sigma_i\ Y_i \rho_i(x,y)/\rho_\infty\ dy \qquad -[11]$$

$$\hat{dx} = dx \qquad -[12]$$

where the variables are the same as for equations [1] - [4] and $Y_i$ is the mass fraction for species i

## Description of Experiments

A series of experiments were run in the T3 shock tunnel facility at A.N.U. Canberra involving the injection of hydrogen into supersonic co-flowing air streams. The nominal Mach number of the free stream air flow was 3.5. A schematic diagram of the experimental configuration is given in figure 3 where it can be seen that the flow of hydrogen was injected into a 25mm x 50mm duct. Care was taken to avoid unnecessary compressive and expansive waves from being present inside the duct as these would negate the two dimensionality of the flow. Furthermore, the flow was considered to be two dimensional free mixing up until the point where the compression waves from the injector entered the mixing region after reflecting off the side walls as shown in figure 3 .

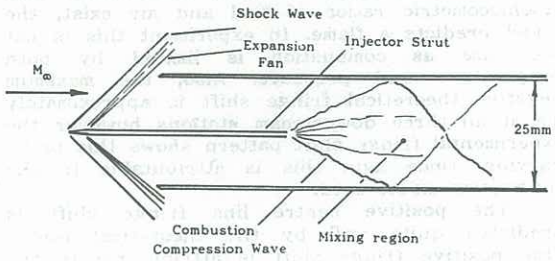


Figure 3 Experimental set up

An interferogram taken from this facility is given in figure 4. This demonstrates the development of the mixing region immediately downstream of the injector which can be seen at the top of the figure. The flow direction is from top to bottom. The compression wave generated off the injector is evident above and below the injector. Also, the wall boundary layers can be seen from the curved fringes near the wall and these can be seen to be small compared to the total width of the duct.

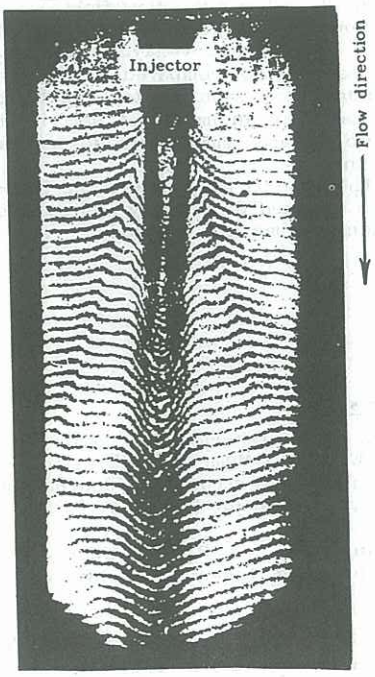


Figure 4 Example interferogram taken From the T3 facility

## Interferogram Prediction

Interferograms are generated by splitting a beam of light and passing one beam through a test section of interest while the other beam circumvents it. The two beams are then rejoined and the the difference between their phases causes either constructive interference or destructive interference of the beam resulting in a fringe pattern. This is shown in figure 5. Density differences in the test section causes phase shifts in the beam of light passing through it as density differences vary the speed of light along the optical path. As shown in figure 5, mirrors b and d are half silvered so as to allow half of the incident light to be reflected and the other half passes through the mirror.

Fringe shift predictions can be made by making use of the Gladstone Dale formula given in equation [13]. Here, F is the value of the fringe shift, $\rho_i$ is the density of species i, $\xi_i$ is the value of the Gladstone Dale constant for species i, L is the optical path length as shown in figure 4 and $\lambda$ is the frequency of the light source.

$$F = \Sigma_i \rho_i \xi_i L Y_i / \lambda \qquad -[13]$$

By combining equation [13] above with the equations to solve for the flow fields, an estimate of the interferogram can be produced. These predicted fringe shift profiles were implemented computationaly by the methods thus far described. A comparison between an experimental fringe shift pattern and the corresponding theoretical pattern is given in figure 5. The test conditions which generated the experimental pattern are listed in table 1. Furthermore, the expected pattern for a flow with the test conditions listed in table 2 is given in figure 6. This flow is of Mach number 5.2. Two points should be noted; 1) variations in the optical path length between the two beams preceding the disturbances in the test section will vary the number of fringes in the field of view of any interferogram, 2) misallignment in the mirrors of the interferometer determine which direction the fringe pattern will shift for a given positive density change.

Hence, it is the relative fringe shift magnitude along any fringe which is important as the direction of the fringe shift is a parameter of the experimental set up only.

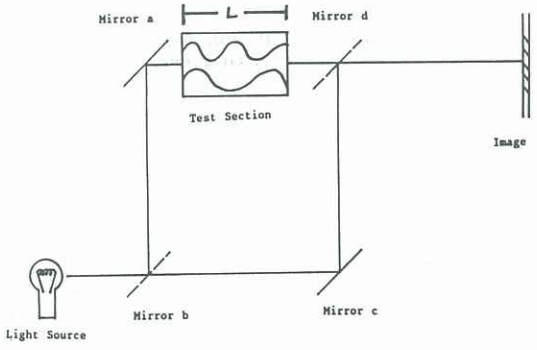


Figure 5 Schematic diagram of the interferometer

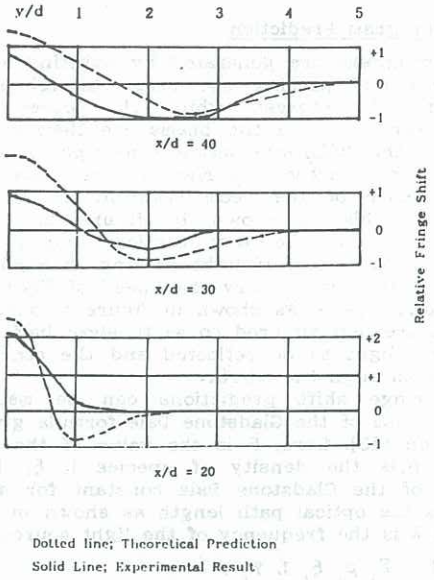


**Figure 6 Comparison between theory and experiment for the fringes of the interferograms**

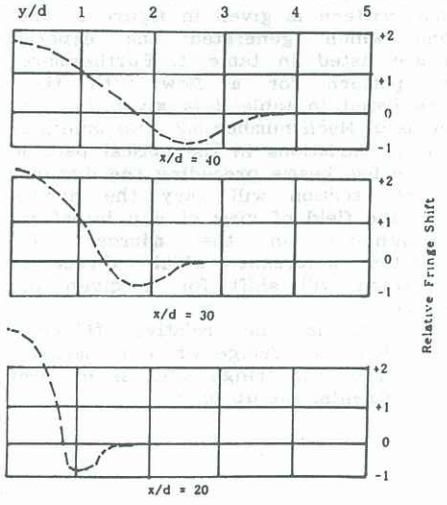


**Figure 7 Fringe prediction for the hypersonic mixing case**

| | Table 1 | Table 2 |
|---|---|---|
| Air Temp. (K) | 3078 | 2000 |
| Air Vel. (m/s) | 3785 | 4500 |
| Air Dens. ($kg/m^3$) | 0.126 | 0.125 |
| Hyd. Temp. (K) | 248 | 248 |
| Hyd. Vel. (m/s) | 1200 | 1200 |
| Hyd. Dens. ($kg/m^3$) | 0.129 | 0.129 |

## Conclusions

The predicted fringe pattern gave a reasonable estimate to the experimental fringe pattern in both shape and size. That is to say that the relative magnitude of the fringe shifts were comparable as well as the location of the fringe shifts in the x and y directions. The predicted fringe pattern did give a slightly erroneous prediction close to the injector as can be seen in figure [6] for x.d = 20. In this case the maximum negative theoretical fringe shift is approximately 0.8 whilst the experimental fringe pattern does not register a negative fringe shift. This discrepancy can be attributed to the Schwarb Zeldovich combustion model used. This model has no limits on combustion so that everywhere that stochiocometric ratios of fuel and air exist, the model predicts a flame. In experiment this is not the case as combustion is limited by both temperature and pressure. Also, the maximum negative theoretical fringe shift is approximately 0.8 at all three downstream stations however the experimental fringe shift pattern shows this to be varying. Once agin this is attributable to the combustion model used.

The positive centre line fringe shift is predicted quite well by the theoretical model. This positive fringe shift is attributable to the presence of low density, low temperature hydrogen. As these diffuse away from the centre of the mixing region the increase in temperature tends to reduce density whilst the outward diffusion of hydrogen tends to increase the density and so the resulting fringe shifting due to these two affects is partially negated. Thus the "flattening out" of the fringe profile mat appear slower than expected as downstream distance is increased.

Several improvements can be made to the model; 1) the spreading coefficient used was derived from Weinstein's (1956) experiments. It would be more accurate to generate such a profile as in figure 2 for the experimental case being investigated. However in order to solve the equations necessary to generate this plot, empirical data must be used which is tantamount to experimentally solving the flow field,

2) boundary layers were not include in the flow. The wall boundary layers were seen from figure 4 to be small compared to the duct width. The boundary layers on the top and bottom of the injector may play an important part in the mixing of the two streams immediately downstream of the injector and

3) The prandtl number and the Lewis number were both assumed to be unity and so relaxing this assumption will improve the model.

## References

Weinstein, A.S., Osterle, J.F, and Forstall, W. (1956) Momentum diffusion from a slot jet into a moving secondary. Journal of Applied Mechanics, Sept. 56 pp 437 -443.

Forthmann, E. (1934) Uber turbulente strahlausbreitung. Ingenieur Archiv, vol. 5 p 42

Kanury, A. (1975) Introduction to Combustion Phenomena. Gordon and Breach, N.Y.